Macromolecules

Article

Cite This: Macromolecules 2019, 52, 6416−6427

pubs.acs.org/Macromolecules

Kinetics of Mesoglobule Formation and Growth in Aqueous Poly(*N*-isopropylacrylamide) Solutions: Pressure Jumps at Low and at High Pressure

Bart-Jan Niebuur,[†] Leonardo Chiappisi,[‡,§] Florian Jung,[†] Xiaohan Zhang,[†] Alfons Schulte,*[,∥] and Christine M. Papadakis*[,†]

[†]Physik-Department, Fachgebiet Physik weicher Materie, Technische Universität München, James-Franck-Straße 1, 85748 Garching, Germany

[‡]Large Scale Structures Group, Institut Laue-Langevin, 71, Avenue des Martyrs, 38042 Grenoble, France

[§]Stranski Laboratorium für Physikalische und Theoretische Chemie, Institut für Chemie, Technische Universität Berlin, Straße des 17. Juni 124, Sekr. TC7, D-10623 Berlin, Germany

[∥]Department of Physics and College of Optics and Photonics, University of Central Florida, 4111 Libra Drive, Orlando, Florida 32816-2385, United States

Supporting Information

ABSTRACT: The mesoglobule formation and growth in an aqueous solution of poly(*N*-isopropylacrylamide) are investigated using time-resolved small-angle neutron scattering. Rapid pressure jumps initiate phase separation at both low (below 20 MPa) and high pressures (above 101 MPa). Measurements were carried out in a time range from 50 ms to ∼1650 s after the jump, covering a large range of momentum transfers. The dehydration of the polymer at the coexistence line is much stronger at low pressures than at high pressures, which significantly affects the mechanism of phase separation: At low pressures, the diffusion-limited coalescence of the mesoglobules is strongly slowed down by the viscoelastic effect due to their dense shell. Moreover, the target pressure has a strong influence on the relative importance of these kinetic effects. In the high-pressure regime, the viscoelastic effect does not play a role, and diffusion-limited coalescence proceeds without hindrance.

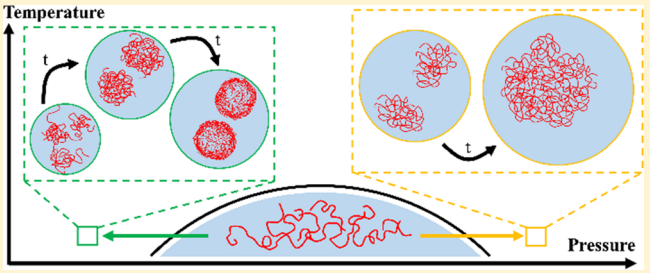

INTRODUCTION

The mechanisms of growth in aggregating systems as well as interactions stabilizing the aggregates are of great importance in a wide variety of research areas, including the study of synthetic polymers and proteins.[1] Moreover, they are of relevance to gain insights into the rational design of smart materials.[2−4] The aggregate formation of stimuli-responsive polymers is of special interest since their solubility can be drastically altered by external stimuli, such as temperature, light, ionic strength, or pressure, resulting in collapse and aggregation.[5−8]

A well-studied model polymer in this respect is poly(*N*-isopropylacrylamide) (PNIPAM), which reacts distinctly to changes in temperature or pressure. At atmospheric pressure, aqueous solutions of PNIPAM feature a lower critical solution temperature at ∼32 °C.[9] Hydration water, that is, water that interacts closely with the chains, is released at the phase transition,[10,11] leading to a sharp coil-to-globule transition of the individual chains.[12,13] The kinetics of this transition was studied in detail. In agreement with theoretical predictions,[14−16] it was shown that the coil-to-globule transition in dilute PNIPAM solutions is a two-step process that can be attributed to the local contraction of chain segments ($\tau \cong 0.1$ ms) followed by their merging and coarsening ($\tau \cong 0.5-1$ ms).[17−19] In semidilute solutions, a third stage was observed and was related to a disentanglement process of overlapping chains.[20]

On longer timescales, the subsequent aggregation of the collapsed PNIPAM chains results in the formation of long-lived aggregates in the mesoscopic size range, termed mesoglobules.[21−23] Their size depends on polymer concentration,[21,24,25] polymer molar mass,[21] quenching temperature,[26] heating rate,[24,27] ionic strength of the solvent,[25] and pressure.[10] Several mechanisms have been proposed to contribute to their stability. Due to the amphiphilic nature of the PNIPAM monomers, hydrophilic groups may accumulate at the surface of the mesoglobules, thereby reducing their interfacial tension with respect to water and enhancing their stability.[21,23,28−30] A second proposed mechanism considered the accumulation of charges at the surface of the mesoglobules, which results in a repulsive force, hindering aggregation.[26] Furthermore, it has been argued that the chain entanglement time is much longer

Received: May 6, 2019
Revised: July 27, 2019
Published: August 19, 2019

DOI: 10.1021/acs.macromol.9b00937
Macromolecules 2019, 52, 6416−6427

than the time during which two mesoglobules are in contact, thereby reducing the probability of coalescence and leading to an entanglement force that prevents macrophase separation in the solution.[27,31,32] Since the chains strongly dehydrate when the cloud point (CP) is traversed at atmospheric pressure, the chain mobility in the mesoglobules is low, which leads to a pronounced viscoelastic effect.[10] Few studies have aimed at investigating the kinetic pathway of mesoglobule formation in aqueous PNIPAM solutions, following a temperature jump across the CP.[24,33,34] Employing time-resolved (kinetic) small-angle neutron scattering (SANS) with a time resolution of ∼100 s, it was observed that the growth of mesoglobules in a concentrated aqueous PNIPAM solution is at least a two-stage process.[33] However, the SANS data in the initial stages were obscured by the rather long time needed for heating the large sample volume and by temperature gradients.

As an alternative to temperature, pressure jumps can be applied to induce phase separation. Furthermore, experiments in different pressure regimes offer the possibility to control the degree of dehydration and thus the viscoelastic effect. It was previously observed that the dehydration at the CP is much weaker at high pressures.[10,35] This has been attributed to the reduction of the hydrophobic effect at high pressure that has been primarily studied in protein solutions.[36−39] However, additional mechanisms may play a role as well, such as the tightness of the solvation shell.[40] When the CP is crossed at high pressure, the chains in the mesoglobules remain more mobile, which may lead to a pathway different from the case of strong dehydration and immobile chains. Using very small-angle neutron scattering, we found that, at high pressure (80−113 MPa), the mesoglobules are much larger and contain more water than at atmospheric pressure.[10] To discriminate the influence of dehydration, hydrophobic interactions, and the viscoelastic effect on the pathway of mesoglobule formation, it is thus of interest to investigate the kinetics of the phase transition in different pressure regimes. This is in the focus of the present investigation.

In our recent work,[41] we addressed the low-pressure (LP) regime of a PNIPAM solution in D_2O (3 wt %) by combining fast pressure jumps to initiate phase separation and kinetic SANS to investigate the time course of mesoglobule formation. Similar to previously reported studies,[42−45] fast pressure jumps were initiated by rapidly opening a pneumatically driven valve between the pressure cell and a reservoir, resulting in a time resolution better than 0.1 s. An advantage of this method over systems based on piezoelectric actuators is that large sample volumes can be employed and that the amplitudes of the jumps can be varied over a larger range.[46−48]

Starting in the one-phase region at 31 MPa and at 35.1 °C, the pressure was rapidly lowered by 15 or 21 MPa, crossing the coexistence line of the one-phase and two-phase regions, toward an endpoint in the two-phase region. Three regimes of growth were identified: During the first ∼1 s, fractal clusters of chains are formed that subsequently become compact, resulting in mesoglobules. These grow by diffusion-limited coalescence. After 10−30 s, a dense PNIPAM shell around the mesoglobules emerges due to the diffusion of water out of the near-surface layer. This shell hinders further coalescence of mesoglobules, resulting in an energy barrier of several k_BT. At later times (at least up to ∼1600 s), the growth proceeds extremely slowly. The characteristic times were found to depend on the target pressure, that is, on the jump amplitude. Thus, it is of interest to follow the behavior at even smaller and at larger amplitudes of the jumps to focus on the different stages of growth. The kinetics resulting from jumps with smaller and larger amplitudes is described in detail in the present paper.

Moreover, pressure jumps in the high-pressure (HP) regime of the phase diagram allow us to elucidate the chain collapse and mesoglobule growth in the regime where dehydration is weak and where the chains stay more mobile than at low pressures. To this end, we carried out pressure jumps in the high-pressure regime (above 100 MPa) at the same temperature, crossing the coexistence line at high pressures. A series of pressure jumps were conducted starting from the same initial pressure of 87 MPa. The initial pressure was chosen so as to have a similar pressure difference from the coexistence line as for the jumps in the LP regime. Varying the target pressure in the two-phase region allows us to characterize the formation and growth of mesoglobules.

This article is organized as follows: Following the Introduction, the description of the sample and the technical details of the pressure jump experiments are given in the Experimental Section. The Results and Discussion section presents the detailed analysis of the kinetics of mesoglobule formation in the LP regime and in the HP regime. The findings in both pressure regimes are summarized in the Conclusions.

EXPERIMENTAL SECTION

Materials. Poly(*N*-isopropylacrylamide) (PNIPAM) with M_n = 36 kg mol^{-1} and $Đ$ = 1.26 (end groups carboxylic acid and a hydrogen atom) was purchased from Sigma-Aldrich. Prior to the measurements, PNIPAM was dissolved in D_2O (Deutero, 99.95%) at a concentration of 3 wt %, which is in the semidilute concentration regime. The solutions were shaken for at least 48 h at room temperature.

Time-Resolved Small-Angle Neutron Scattering (TR-SANS). TR-SANS experiments were performed at the instrument D11 at the Institute Laue-Langevin (ILL), Grenoble, France, along the lines described previously using the same calibration measurements and applying the same raw data treatment.[41] In brief, a neutron wavelength of λ = 0.6 nm with a spread $\Delta\lambda/\lambda$ = 0.09 was selected. The measurements were performed with sample−detector distances (SDDs) of 1.5, 8.0, and 34.0 m, resulting in a range of momentum transfers q of 0.02−3.3 nm^{-1}, with $q = 4\pi \times \sin(\theta/2)/\lambda$, where θ is the scattering angle.

The setup for pressure jumps was described previously (Figure 1a),[41] and it is conceptually similar to that in X-ray scattering studies.[43,44] The pressure cell and the separator (section 2 in Figure 1a) are connected to the external pressure system (section 1 in Figure 1a), including the pressure generator, by a pneumatically driven valve. The separator prevents mixing of the pressure-transmitting medium (3M Fluorinert 770) and the sample. Before each jump, the pneumatically driven valve was kept open, and the system was equilibrated for ∼30 min in the one-phase region.

The protocol of the pressure jump experiments is illustrated in Figure 1b. After setting the pressure to the desired initial value, the pneumatically driven valve was closed, and the pressure in the external system was set to a lower or higher value. The system was equilibrated for 5 min, and a static SANS measurement (prejump measurement) with a measuring time of 1 min was carried out. The pressure jump was performed by a rapid opening of the pneumatically driven valve after which the pressure in both sections of the system equilibrates. A transistor-transistor logic (TTL) pulse, initiated by the opening of the valve, triggered the start of the data acquisition and was found to result in good reproducibility. The frame duration was successively increased after each frame by a factor of 1.1, starting with 0.05 s. After each pressure jump, 85 frames were recorded, which implies a total measuring time of 1649 s. The measurement at SDD = 34 m was repeated at least five times for each jump to obtain sufficient statistics. Selected measurements shortly after the pressure jumps were averaged to improve statistics to allow reliable fits. The time resolution of the

DOI: 10.1021/acs.macromol.9b00937
Macromolecules 2019, 52, 6416−6427

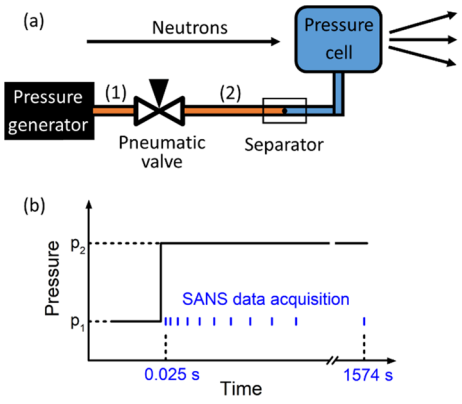

Figure 1. (a) Schematic representation of the pressure system used for the pressure jump experiments. Section 1 is the external system, which includes the pressure generator. Section 2 is connected to section 1 by the pneumatically driven valve and includes the separator and the pressure cell. The separator hinders mixing of the pressure transmitting medium (orange) and the sample (blue). (b) Schematic representation of the protocol of the kinetic SANS experiment after a pressure jump. After equilibration of the sample at pressure p_1, the pressure is rapidly increased or decreased to pressure p_2. The start of the SANS data acquisition is triggered by opening the valve, and the first frame has an acquisition time of 0.05 s; that is, the mean time after the jump is 0.025 s. The acquisition time is increased by a factor of 1.1 after each frame until the last frame at 1574 s.

experiment is limited by the response time of the pneumatically driven valve, which is less than 0.05 s, and the flight time of the neutrons between the sample and the detector, which amounts to ~0.05 s at the longest SDD of 34.0 m, as derived from the wavelength of the neutrons.

The coexistence line of a 3 wt % PNIPAM solution in D_2O in dependence on temperature and pressure has an elliptical shape (Figure 2),[41] similar to results from PNIPAM solutions with different polymer

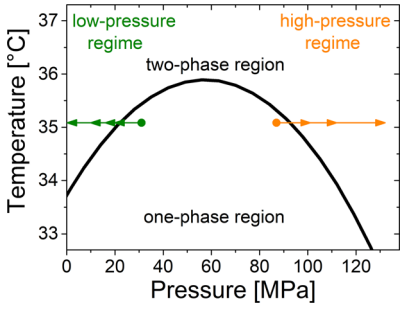

Figure 2. Pressure−temperature phase diagram of the 3 wt % PNIPAM solution in D_2O, as determined by turbidimetry,[41] in the region of interest for the pressure jump experiments. The arrows indicate the start and the target pressure of the jumps in the LP regime (green arrows) and the HP regime (orange arrows).

concentrations and molar masses.[49−51] At atmospheric pressure, the CP is at 33.7 °C, and a maximum of 35.9 °C is encountered at ~60 MPa. At temperatures in between, the CP is traversed twice with varying pressure, which allows investigations of the kinetics of mesoglobule formation both, at low and at high pressure, at the same temperature. For the pressure jumps, a temperature of 35.1 °C was chosen; the CPs are then located at 21.8 ± 2.5 and 89.6 ± 1.0 MPa, as found with static SANS measurements during a pressure scan (see the Supporting Information for details). The initial pressure for the jumps in the LP regime was chosen at 31.0 MPa, that is, 9.2 MPa above the coexistence pressure, whereas it was 87.0 MPa for the jumps in the HP regime, that is, 2.6 MPa below the coexistence pressure. In the LP regime, jumps were performed by decreasing the pressure to four different target pressures in the two-phase region, with pressure changes $\Delta p = -11$, -15, -21, and -31 MPa, as indicated in Figure 2. In the HP regime, jumps were performed by increasing the pressure to three different target pressures in the two-phase region with pressure changes $\Delta p = 14$, 25, and 45 MPa (Figure 2).

SANS Data Analysis. The data analysis was carried out as described previously:[41] In the one-phase region, the Ornstein−Zernike structure factor[52] was used to describe the concentration fluctuations in the one-phase region. It contains the correlation length of concentration fluctuations ξ, which is assigned to the average distance between entanglement points.[53] Its amplitude I_{OZ} corresponds to the contribution from concentration fluctuations to the scattered intensity at $q = 0$.

In the two-phase region, a superposition of the Ornstein−Zernike structure factor, again describing concentration fluctuations on small length scales, and a form factor $I_{agg}(q)$ to account for the scattering from aggregates was used to model the scattering curves, similar to previously published works.[54,55] Thus, after the pressure jumps, the scattering curves were fitted by the model

$$I(q) = I_{agg}(q) + I_{OZ}(q) + I_{bkg} \quad (1)$$

Two form factors were used to describe $I_{agg}(q)$: In the LP regime, the aggregates were rather small, and their size could be determined using the Guinier−Porod form factor.[56] It contains the radius of gyration of the aggregates R_g and the intensity at $q = 0$, I_{agg}. Moreover, it contains the Porod exponent m associated with the surface structure of the mesoglobules. For smooth surfaces, $m = 4$, whereas for rough surfaces, $3 \leq m \leq 4$. An SLD gradient perpendicular to the surface of the mesoglobules results in an apparent $m > 4$.[57,58] Weak interaction between mesoglobules may be present. However, the covered q range does not allow its characterization. Also, in the two-phase region, the Ornstein−Zernike structure factor was used to describe concentration fluctuations on small length scales, which may originate from individual chains, small clusters of chains, and inhomogeneities inside mesoglobules.

In the HP regime, the size of the aggregates was too large to be resolved. Their scattering contribution was therefore parametrized by the Porod form factor.[59] It contains the Porod amplitude I_P and the Porod exponent m, allowing extraction of information about the surface structure of the mesoglobules (see above). The Ornstein−Zernike structure factor accounts again for concentration fluctuations on small length scales. In all cases, the incoherent background I_{bkg} was added as a floating parameter. In the Supporting Information, the full expressions of the fitting functions are given. Standard procedures were applied to account for smearing due to the divergence of the neutron beam and the wavelength distribution.[60]

RESULTS AND DISCUSSION

In this section, we first describe the structures of the 3 wt % PNIPAM solution in D_2O in the initial states. We then proceed to the description of the mesoglobule formation in the low- and the high-pressure regimes. For consistency, the same polymer concentration as in our previous study was employed, which is in the semidilute regime.[41] D_2O is used as a solvent to optimize the contrast for neutron scattering between the different phases. We believe that the overall findings are applicable to the more commonly used H_2O.[61] The results are discussed in terms of thermodynamic driving forces and kinetic hindrances.

Initial State in the One-Phase Region. The SANS data recorded at the prejump pressures in the LP and the HP regimes are depicted in Figure 3a. The curves show a decay above ~0.04 nm^{-1}, characteristic of semidilute polymer solutions in the one-phase region. Furthermore, additional weak forward scattering is observed below 0.04 nm^{-1}, which indicates the presence of inhomogeneities at larger length scales.

Two models were used to fit the scattering curves. First, the Ornstein−Zernike structure factor (eq S2), describing the

DOI: 10.1021/acs.macromol.9b00937
Macromolecules 2019, 52, 6416−6427

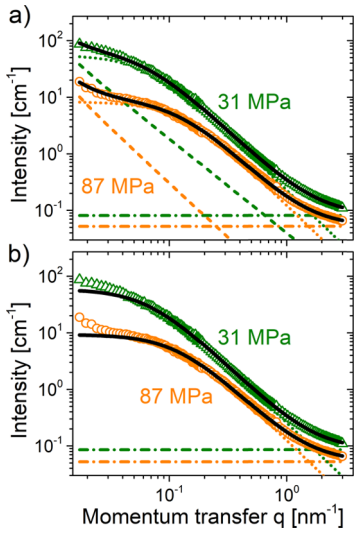

Figure 3. SANS curves recorded prior to the pressure jumps at 31 MPa and 35.1 °C (LP regime, green symbols) and 87 MPa and 35.1 °C (HP regime, orange symbols) modeled by a combination of the Porod form factor and the Ornstein−Zernike structure factor (a) and solely by the Ornstein−Zernike structure factor (b). Solid black lines: fits, dashed lines: Porod form factor, dotted lines: Ornstein−Zernike structure factor, dashed-dotted lines: incoherent background.

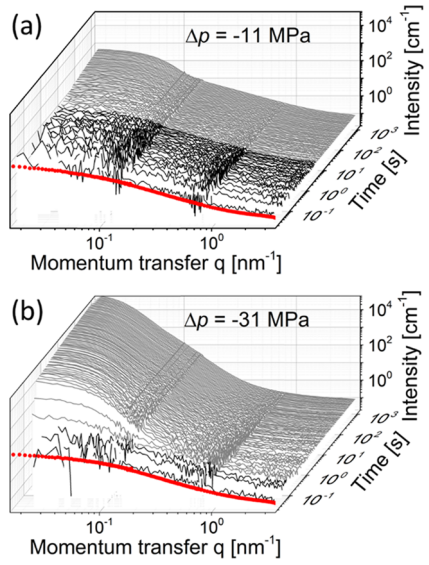

Figure 4. SANS curves of the 3 wt % PNIPAM solution in D_2O in the LP regime after jumps starting at T = 35.1 °C and p = 31 MPa with pressure changes of Δp = −11 (a) and −31 MPa (b). Red symbols: prejump measurements, black and gray lines indicate the curves that are fitted without and with the contribution $I_{agg}(q)$ in eq 1, respectively.

concentration fluctuations at a local scale, was combined with the Porod form factor (eq S7), accounting for the forward scattering due to large-scale inhomogeneities (Figure 3a). The resulting correlation lengths at 31 and 87 MPa are ξ = 15.7 ± 0.2 and 8.2 ± 0.1 nm, respectively. In the blob model,[53] ξ is the average distance between the overlap points of the chains. Thus, the chain conformation is slightly different at high pressure: The lower value of ξ at 87 MPa points to a higher density of overlap points[62] and, therefore, to a more expanded chain conformation, which may be assigned to the higher degree of hydration of PNIPAM at high pressure. It may also be due to the smaller pressure difference from the coexistence line compared to 31 MPa.[63] The Porod exponents, accounting for large-scale inhomogeneities, are m = 1.6 ± 0.1 and 1.9 ± 0.1 at 31 and 87 MPa, respectively, which shows that they are loose fractal-like structures. Second, solely the Ornstein−Zernike structure factor was employed to fit the data at q values above 0.04 nm^{-1} (Figure 3b), resulting in correlation lengths ξ = 15.2 ± 0.1 nm at 31 MPa and 8.6 ± 0.1 nm at 87 MPa. These values are very similar to the ones given above. Furthermore, the values of I_{OZ} obtained with both fitting models are very close to each other. In the kinetic experiments described below, no forward scattering can be identified at short times after the jump (presumably because of the rather high noise at short timescales), and the values from the second approach (Ornstein−Zernike fit) are used in the following. All resulting fitting parameters are shown in Figures 6 and 10.

Mesoglobule Formation in the Low-Pressure Regime. As discussed in our previous paper[41] and in the Introduction, three growth regimes are encountered after the jumps with pressure changes Δp = −15 and Δp = −21 MPa, namely, the formation of fractal clusters of chains and their compactification, resulting in mesoglobules. These grow first by diffusion-limited coalescence until a dense PNIPAM shell is formed, hindering further coalescence and leading to a strong slowing down of the growth.[41] Figure 4 displays the SANS curves following the jumps starting at 31 MPa with pressure changes Δp = −11 and −31 MPa, that is, in the LP regime. Immediately after the jump with Δp = −31 MPa, the SANS curves feature a shoulder, which increases slightly in intensity. After 0.17 s, a second contribution in the low$q$ range is discernible (below 0.1 nm^{-1}), which abruptly increases in intensity, indicating the sudden formation and growth of mesoglobules. This happens later than at Δp = −15 and −21 MPa. After 0.4 s, that is, very soon after mesoglobule formation, the slow growth regime is entered as well.

The jump with the smallest amplitude (Δp = −11 MPa, Figure 4a) gives qualitatively different results: At short timescales, merely small changes in the scattering curves are observed. Only after 7.9 s, an increase in intensity at low q values (below 0.1 nm^{-1}) is discernible, pointing to the formation of large structures. The increase is, however, much weaker than for jumps with a larger amplitude.

For all pressure jumps, there are only weak changes in the scattering curves at high q values. The shoulder observed in the prejump measurement, assigned to concentration fluctuations of the polymer solution, persists even after mesoglobules are formed. Thus, concentration fluctuations at small length scales are present after mesoglobule formation.

To extract quantitative structural information, the scattering curves are modeled by the superposition of the Ornstein−Zernike structure factor, the Guinier−Porod form factor, and the incoherent background (eq 1 and eqs S1−S6). A comparison between data and fitted curve is exemplarily shown in Figure 5. After the pressure jumps, the chains collapse and form small clusters. However, the quality of the data was insufficient to distinguish the weak excess forward scattering observed in the one-phase region (Figure 3), and $I_{agg}(q)$ was therefore set to zero. The Ornstein−Zernike structure factor is used as the simplest possible model to extract the correlation length ξ and the amplitude I_{OZ}. As soon as scattering from concentration fluctuations and mesoglobules can be distinguished from each other, the Guinier−Porod form factor is included as well. It comprises the radius of gyration of the mesoglobules R_g and the

DOI: 10.1021/acs.macromol.9b00937
Macromolecules 2019, 52, 6416−6427

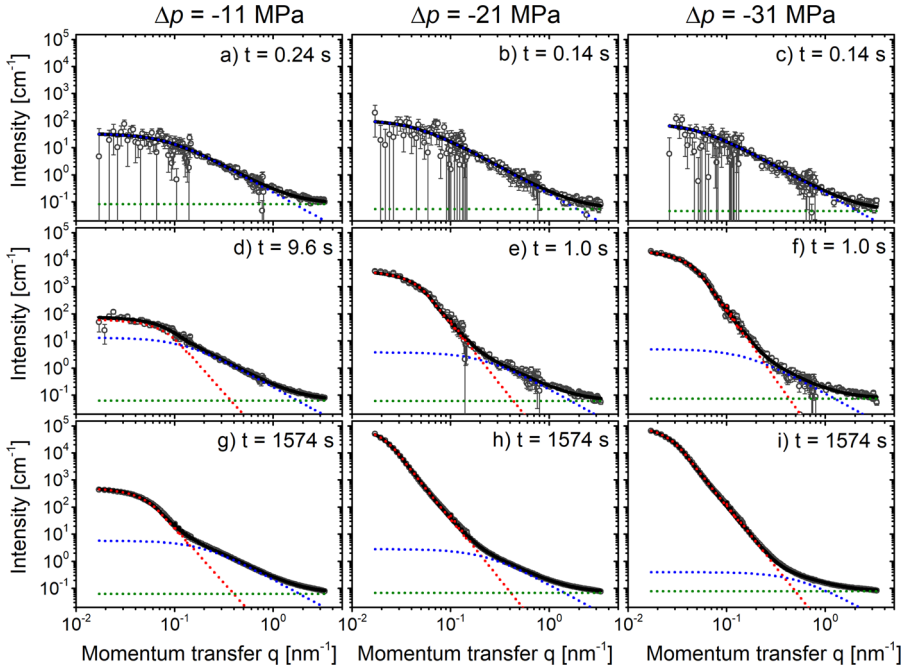

Figure 5. Representative SANS data (symbols) in the LP regime along with model fits for $\Delta p = -11$ (a,d,g), -21 (b,e,h), and -31 MPa (c,f,i) at three different times after the jump, as indicated in the graphs. The solid lines are fits of eq 1 (see text for details). Red dotted lines: $I_{agg}(q)$, blue dotted lines: $I_{OZ}(q)$, olive dotted lines: I_{bkg}.

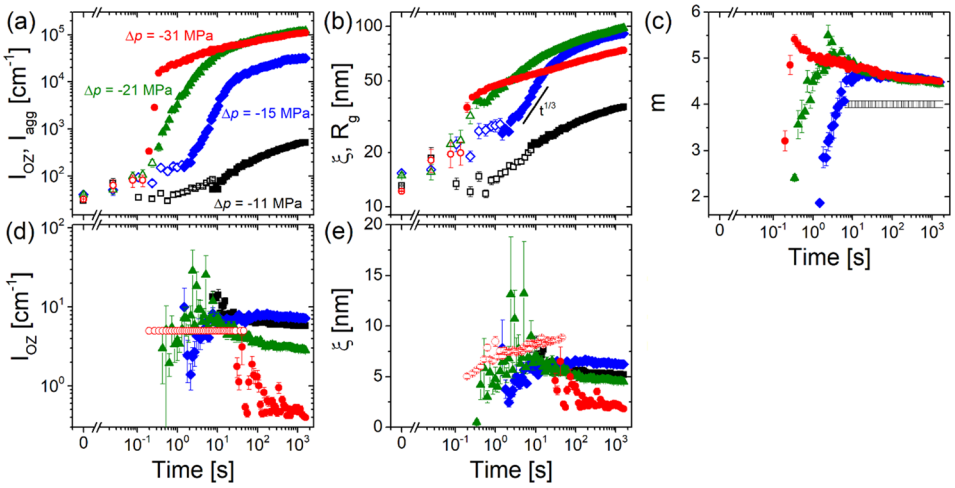

Figure 6. Results from fits to the scattering curves in the LP regime. (a) Amplitudes of the Ornstein–Zernike structure factor I_{OZ} (open symbols) and of the Guinier–Porod form factor I_{agg} (closed symbols), (b) correlation length of concentration fluctuations ξ (open symbols) and radius of gyration R_g (closed symbols), (c) Porod exponent m, (d) amplitudes of the Ornstein–Zernike structure factor I_{OZ} at later times, and (e) correlation length of concentration fluctuations ξ at later times. Black squares: $\Delta p = -11$ MPa, blue diamonds: $\Delta p = -15$ MPa, green triangles: $\Delta p = -21$ MPa, and red circles: $\Delta p = -31$ MPa. The results for $\Delta p = -15$ and -21 MPa are taken from ref 41. The open symbols in panels (c–e) represent data that were kept at a fixed value or data that are directly affected by fixation of parameters during fitting and are thus not trustworthy (see text for details).

Porod exponent m, characteristic of their surface structure (see the Supporting Information).

The time dependence of the resulting fitting parameters is shown in Figure 6 for all runs in the LP regime. The behavior of the lengths and scattering intensities confirms the visual observations from the scattering curves. Directly after the jumps, mesoglobules have not formed yet, and the solutions are still in the one-phase region. The significant increase of I_{OZ} after the jumps with $\Delta p = -15$, -21, and -31 MPa (Figure 6a) shows that concentration fluctuations become more pronounced. ξ behaves similarly (Figure 6b): ξ increases steadily from the initial (prejump) value of ∼15 to ∼25 nm within 0.1 s after the jumps with $\Delta p = -15$, -21, and -31 MPa. It can be expected that, due to the relatively high polymer concentration of 3 wt %, which is above the overlap concentration,[41] chains tend to cluster together during the early stages after the pressure jump.[20] These clusters are the building blocks for the mesoglobules. For $\Delta p = -11$ MPa, cluster formation is significantly slower. Directly after the jump, I_{OZ} and ξ stay constant, and only after ∼0.5 s, an increase in both quantities is observed.

After 7.9, 1.4, 0.3, and 0.17 s for $\Delta p = -11$, -15, -21, and -31 MPa, respectively, the intensity I_{agg} (Figure 6a), which is assigned to scattering from the mesoglobules, continues the increasing trend of I_{OZ} directly after the jump. However, it

DOI: 10.1021/acs.macromol.9b00937
Macromolecules 2019, 52, 6416–6427

increases more rapidly for $\Delta p = -15$, -21, and -31 MPa. The nearly continuous trend of I_{OZ} and I_{agg} shows that, starting immediately after the jumps, the scattering from clusters becomes increasingly more important with time and dominates over the scattering from concentration fluctuations (a small discontinuity between both quantities may be due to the alteration of the model used for fitting). At later times (after ∼30 s for $\Delta p = -15$ MPa, ∼10 s for -21 MPa, and 0.4 s for -31 MPa), the increase of I_{agg} is slowed down; that is, an earlier onset occurs for larger Δp. Changes in the system are therefore less pronounced at later times. In contrast, for the jump with $\Delta p = -11$ MPa, I_{agg} only increases very slowly during the entire time, presumably due to a low thermodynamic driving force for phase separation.

These findings are corroborated by the behavior of the radius of gyration of the mesoglobules R_g shown in Figure 6b. It continues the increasing trend of ξ directly after the jump but at a much higher rate. We note that, at this stage, phase separation is probably not yet completed. The chains are still hydrated to a certain degree and thus highly mobile. Rearrangements of chains or clusters of chains are still possible, allowing a rapid growth. As discussed previously for the jumps with $\Delta p = -15$ and -21 MPa,[41] the high mobility of chains during the early stages of mesoglobule formation allows for rapid growth through coalescence, which is only limited by the diffusion of the mesoglobules. This growth process where the radius is proportional to $t^{1/3}$[64] is only observed for $\Delta p = -15$ and -21 MPa (for a detailed discussion, see ref 41). For the jump with $\Delta p = -31$ MPa, diffusion-limited aggregation is not observed; instead, both I_{agg} and R_g increase very rapidly 0.15−0.3 s after the jump (Figure 6a,b). In this case, the thermodynamic driving force for phase separation is strong, leading to fast dehydration and a large reduction in the mobility of the chains. Thus, the initially very fast growth of the mesoglobules slows down.

For $\Delta p = -11$ MPa, rapid growth is not observed during the entire measured time range. As the target pressure is very close to the cloud point, it can be expected that the thermodynamic driving force for phase separation is weak, leading to the very slow growth of the mesoglobules.

Additional information on the growth behavior of the PNIPAM mesoglobules can be extracted from the time dependence of the Porod exponent m, describing the surface structure of the mesoglobules, shown in Figure 6c. As soon as mesoglobules appear, m rapidly increases from ∼2 to 5−6 and then slowly decreases to ∼4.5 at the end of the run for the jumps with $\Delta p = -15$, -21, and -31 MPa. Thus, the mesoglobules are initially mass fractals with a fractal dimension of ∼2; that is, they feature a loose inner structure and thus they contain water. Only at a later stage, they become more compact. The increase of m to values of 5 and above may be attributed to two different processes: First, the mesoglobule surfaces become smooth, with m changing toward 4. Second, a concentration gradient (resulting in a gradient of the scattering length density) at the surface of the mesoglobules emerges, raising m to values above 4. We have previously attributed the appearance of such a gradient to a dense PNIPAM shell, which arises from fast dehydration of the chains and diffusion of the water out of the surface-near layer, leaving the dense polymer behind.[10,41] The water in the inner part of the mesoglobule is trapped. The time for m to reach its maximum depends strongly on Δp (after 17, 3.4, and 0.34 s for -15, -21, and -31 MPa, respectively) and reflects the time needed for mesoglobule formation. At later times, m decreases toward 4.5. Apparently, water permeates slowly through the shell, and the concentration gradient is equilibrated. This shows also that phase separation continues during the whole time range investigated. For $\Delta p = -11$ MPa, m could not be determined reliably because scattering from concentration fluctuations dominates in the intermediate-q region (see Figure 5d,g). m was therefore fixed at 4, which corresponds to smooth surfaces.

For all jumps, the Ornstein−Zernike structure factor is still necessary to model the data in the high-q region even after mesoglobules have formed. Thus, concentration fluctuations are still present, albeit they are weak. For $\Delta p = -31$ MPa, the Ornstein−Zernike contribution is small and overlaps with the aggregate scattering at intermediate times (Figure 5f); thus, the correlation length and scattered intensity cannot be determined reliably for this jump. Therefore, the value of I_{OZ} was fixed at 5 cm^{-1} up to $t = 30$ s. For all jumps, scattering in the high-q region comprises both inhomogeneities inside the mesoglobules and individual chains in the solution. We hypothesize that, for $\Delta p = -15$, -21, and -31 MPa, the scattering from individual chains after mesoglobule formation is negligible because the thermodynamic driving force for phase separation is strong. The presence of inhomogeneities inside the mesoglobules shows that they contain a significant amount of water.

For $\Delta p = -11$ MPa, I_{OZ} only decreases slightly with time. Water slowly leaves the mesoglobules, and the chains pack more densely. In this case, however, individual chains in the solution presumably contribute to the scattering at high q values as well. I_{OZ} keeps decreasing (in contrast to the leveling off when $\Delta p = -15$ and -21 MPa) and reaches a smaller final value, pointing to a more homogeneous inner structure of the mesoglobules (note that the results may be slightly biased by the proximity of the Ornstein−Zernike structure factor and the Guinier−Porod form factor, Figure 5d, g).

The findings from the intensity I_{OZ} are reinforced by the behavior of ξ at later times (Figure 6e). After rearrangements in the system at early times, ξ levels off, and the final value of ξ decreases with increasing Δp for $\Delta p = -15$, -21, and -31 MPa. This shows that the mesoglobules are denser after large-amplitude jumps; that is, they contain less water. Using infrared spectroscopy, it was previously shown that PNIPAM chains do not dehydrate completely during phase separation by heating through the CP at atmospheric pressure:[65] A certain fraction of hydrophilic groups remain hydrogen-bonded with water rather than forming intra- or interchain hydrogen bonds. Furthermore, recent quasi-elastic neutron scattering (QENS) experiments have demonstrated the presence of strongly arrested water in the two-phase region, which was ascribed to trapped water that forms small pockets inside the mesoglobules.[11,66]

Toward the long times at the end of the run, the mesoglobule growth slows down when $\Delta p = -15$ MPa, -21, and -31 MPa. The reason for the slowing down is the development of an energy barrier that hinders the coalescence between mesoglobules when they collide (see the Supporting Information for more details). This growth process presumably becomes dominant when the chains have lost their mobility due to close packing, at least in the shell of the mesoglobules. Rearrangements of the chains needed for coalescence are no longer possible. Following a large-amplitude jump, the solvent quality is worse than after small-amplitude jumps. Phase separation is therefore faster, and the chains lose their mobility sooner, reducing the time at which the slow growth process starts. As a result, for $\Delta p = -31$ MPa, the mesoglobules are significantly smaller at the starting time of the slow growth process (R_g = 43 nm) than after $\Delta p = -15$ (62 nm) and -21

DOI: 10.1021/acs.macromol.9b00937
Macromolecules 2019, 52, 6416−6427

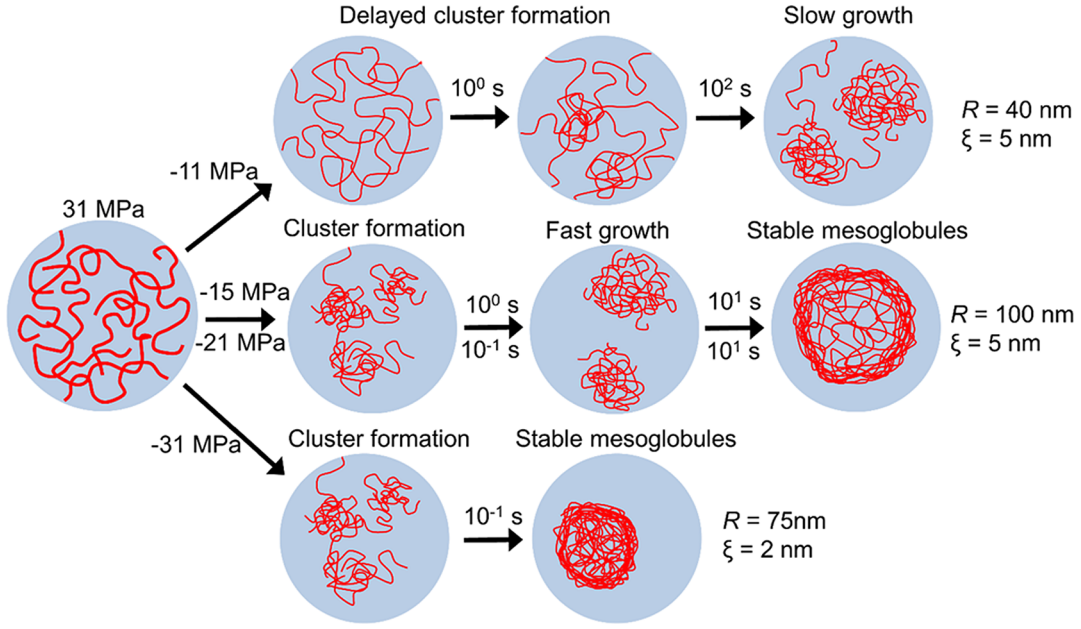

Figure 7. Schematic representation of the different stages of pressure-dependent mesoglobule formation in the LP regime for small-amplitude (−11 MPa), intermediate- (−15 and −21 MPa), and large-amplitude jumps (−31 MPa), with an initial pressure of 31 MPa. The initial pressure and jump amplitude are given on the left, and typical timescales are on the arrows. For details, see text.

MPa (64 nm) where mesoglobules were able to grow without hindrance for a longer time. The detailed time dependence of R_g during this process is determined by Δp: While the transition to slower growth is smooth at −15 MPa, it is more pronounced at −21 MPa and abrupt at −31 MPa. A transition to slower growth is not observed for Δp = −11 MPa on the timescale of the experiment because the mesoglobules still contain a significant amount of water, as seen from the relatively large inner correlation length ξ.

Irrespective of the amplitude of the pressure jump, the mesoglobules continue to grow until the end of the run. The most distinct difference is the final size of the mesoglobules, which does not scale with the amplitude of the jump: At the end of the run, that is, after 1649 s, the size of the mesoglobules is ∼36, ∼92, ∼98, and ∼74 nm for the jumps with Δp = −11, −15, −21, and −31 MPa, respectively. This nonlinear behavior is a result of the combination of several growth processes and their pressure-dependent timescales.

In Figure 7, the dependence of the growth mechanisms on the pressure jump amplitude Δp is schematically summarized. Following a small-amplitude jump (−11 MPa), the formation of clusters immediately after the jump proceeds slowly. These clusters grow continuously until the end of the run, however, with a slow rate. After an intermediate pressure jump (−15 and −21 MPa), clusters form rapidly directly after the jump and grow by diffusion-limited coalescence for a significant time. At later times, the growth is strongly hindered, and large, stable mesoglobules are present, which feature a dense shell. After a large-amplitude jump (−31 MPa), cluster formation directly after the jump proceeds very rapidly beyond the time resolution of the experiment. This results in small, stable mesoglobules already at early times.

Mesoglobule Formation in the High-Pressure Regime. We have previously found that, in the two-phase region at high pressure (at 80 MPa and above), the mesoglobules are significantly larger than at atmospheric pressure, which we attributed to the enhanced hydration of the hydrophobic groups of PNIPAM.[10] It is of interest to investigate the pathway of mesoglobule formation in the HP regime where the chain mobility is less reduced upon phase separation and thus kinetic hindrances are expected to be less prominent than at atmospheric pressure. To this end, pressure jumps were carried out, starting in the one-phase region at 35.1 °C and an initial pressure of 87 MPa (Figure 2). Here, the correlation length of concentration fluctuations amounts to ξ = 8.6 ± 0.1 nm. Large-scale inhomogeneities are present as well, which are more prominent than in the LP regime (Figure 3). Again, the jumps were chosen so as to cross the coexistence line, and their amplitude Δp was varied.

Figure 8 shows the SANS curves before and after the jumps with Δp = 14 (a), 25 (b), and 45 MPa (c). Directly after the jumps, an additional contribution at low q values (q < 0.05 nm^{-1}) appears, which shows that clusters consisting of several chains form immediately. Its slope is still low, which points to the formation of rather loosely packed aggregates. Its intensity increases rapidly, and already after 0.31, 0.17, and 0.11 s for Δp = 14, 25, and 45 MPa, respectively, the contribution due to aggregate scattering is a straight line in the double-logarithmic representation with a slope of approximately q^{-4}, which points to compact and very large mesoglobules, in consistency with our previous static observations.[10] Thus, the time needed for the formation of mesoglobules only decreases slightly with increasing Δp. The maximum intensity that is reached at the lowest q values increases with Δp, pointing to a higher scattering contrast between the polymer-rich and the water-rich phases and thus stronger phase separation for large-amplitude jumps. During the remaining time, the intensity of the aggregate scattering decreases slightly; thus, the mesoglobules grow during the entire run. For none of the jumps, the scattering at high q values (above ∼0.2 nm^{-1}) due to concentration fluctuations decreases significantly with respect to the prejump measurement in dependence on time. This behavior reflects the persistence of strong concentration fluctuations inside the mesoglobules at high pressure, which is in agreement with the relatively strong

DOI: 10.1021/acs.macromol.9b00937
Macromolecules 2019, 52, 6416−6427

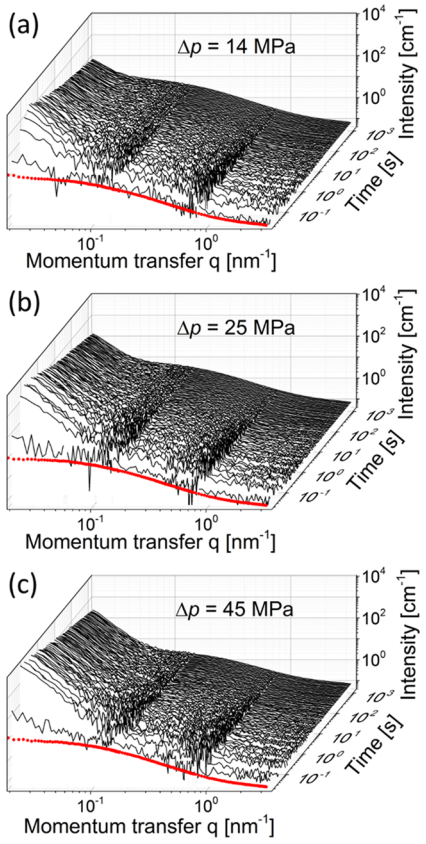

Figure 8. SANS curves of the 3 wt % PNIPAM solution in D_2O in the HP regime after jumps starting at 35.1 °C and p = 87 MPa with pressure changes of Δp = 14 (a), Δp = 25 (b), and Δp = 45 MPa (c). Red symbols: prejump measurements.

hydration of the polymers in the two-phase region, as shown earlier with QENS, SANS, and Raman spectroscopy.[10,11]

To extract quantitative information from the measurements, the SANS curves were again fitted with eq 1, this time with a combination of the Porod form factor, accounting for the scattering from large aggregates (eq S7), and the Ornstein–Zernike structure factor, describing the concentration fluctuations. Figure 9 shows representative scattering curves along with their fits, which are excellent. Only at early times (Figure 9a–c), the forward scattering seems to be a little bent; that is, the aggregates may be rather small. However, the fit with the Guinier–Porod form factor did not lead to reliable results, and therefore, the Porod form factor was used instead, even though it does not allow extraction of the aggregate size.

The time dependences of the characteristic parameters obtained from fits to the scattering curves after the three jumps are presented in Figure 10. Directly after all three jumps, the Porod exponent m (Figure 10a) increases sharply, starting at values of 2–3 and reaching a value of 4 after 0.31, 0.17, and 0.17 s for Δp = 14, 25, and 45 MPa, respectively. Thus, in the HP regime, it takes significantly less time to form well-defined mesoglobules than in the LP regime. This may be due to the weaker dehydration and the resulting higher mobility of the chains. After these times, the value of m was fixed at 4, which gave excellent fits and corresponds to smooth mesoglobule surfaces. (Preliminary fits with a floating value of m resulted in values of 3.7–3.9, pointing to some small surface roughness.) Using the value m = 4 has the advantage that the Porod amplitude K_P can be related to the size of the mesoglobules, which is discussed below.

Since the Ornstein–Zernike structure factor continues to display a significant amplitude even at longer times (Figure 9d–i), concentration fluctuations are still important in the segregated state. I_{OZ}, a measure of the scattering strength from concentration fluctuations, is shown in Figure 10b. While an

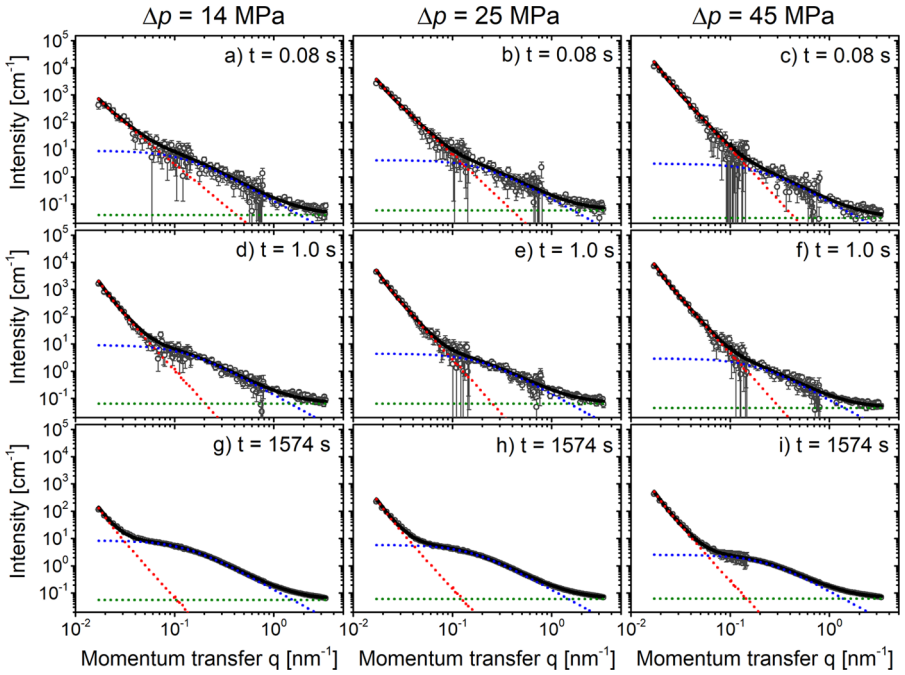

Figure 9. Representative SANS data (symbols) in the HP regime as well as their fits for Δp = 14 (a,d,g), 25 (b,e,h), and 45 MPa (c,f,i) at three different times after the jump, as indicated in the graphs. The solid lines are fits of eq 1 (see text for details). Red dotted lines: I_{agg}, blue dotted lines: I_{OZ}, olive dotted lines: I_{bkg}.

DOI: 10.1021/acs.macromol.9b00937
Macromolecules 2019, 52, 6416–6427

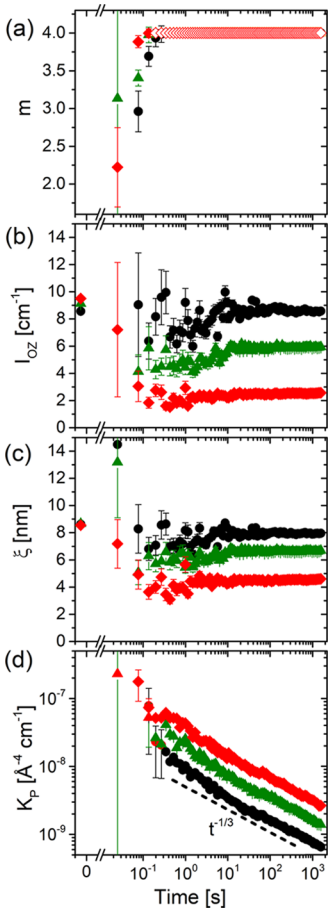

Figure 10. Results from fits to the scattering curves in the HP regime. (a) Porod exponent m, (b) correlation length of concentration fluctuations ξ, (c) amplitude of the Ornstein−Zernike structure factor I_{OZ}, and (d) Porod amplitude K_P. Black circles: Δp = 14 MPa, green triangles: Δp = 25 MPa, red diamonds: Δp = 45 MPa. The open symbols in panel (a) represent data that were kept at a fixed value during fitting (see text for details).

initial decrease of I_{OZ} is observed after all jumps, it is much more pronounced after large-amplitude jumps than after small-amplitude ones. Following all jumps, I_{OZ} increases weakly at later times until it reaches a final value, namely, 8.6, 5.9, and 2.6 cm^{-1} for Δp = 14, 25, and 45 MPa, respectively. Thus, the larger the jump amplitude, the lower is the scattering from inhomogeneities in the mesoglobules and the more homogeneous are the mesoglobules.

The correlation length of concentration fluctuations ξ (Figure 10c) behaves similarly. It traverses through a shallow minimum at ∼0.3 s after the pressure change for all jumps, then increases slightly to a value that depends on Δp (ξ = 8.0, 6.7, and 4.6 nm for Δp = 14, 25, and 45 MPa, respectively), and does not change further during the remaining time. Slight rearrangements may occur during the first 0.3 s, and discontinuous behavior of ξ reflects the complex kinetics resulting from the instant change in interactions caused by the pressure jump. The final values of ξ decrease with the pressure distance of the target pressure from the coexistence line, that is, with decreasing solvent quality: The chain hydration is reduced, and thus, the mesoglobules are denser after large-amplitude jumps. This confirms that the mesoglobules in the HP regime contain a significant amount of water[10] and the chains are strongly hydrated.[10,35]

The Porod amplitude K_P decreases during the entire run for all jumps (Figure 10d). When m = 4, K_P is related to the difference in scattering length densities between the mesoglobules and the solvent $\Delta\rho$ and the specific surface of the mesoglobules S_v by

$$K_P = 2\pi(\Delta\rho)^2 S_v \quad (2)$$

After ∼30 s for Δp = 14 MPa, ∼10 s for Δp = 25 MPa, and ∼2 s for Δp = 45 MPa, ξ reaches its final value. After these times, the inner structure of the mesoglobules does not change anymore, and thus, $\Delta\rho$ can be considered constant. From this point on, K_P decreases, following a $t^{-1/3}$ behavior. As for spherical mesoglobules, $S_V \propto R^{-1}$, the growth of the mesoglobules follows $R \propto t^{1/3}$, which is consistent with the growth by diffusion-limited coalescence.[64] This result shows that, in contrast to the LP regime, there is no energy barrier hindering coalescence at later times. The mesoglobules grow continuously, and no mechanism preventing macroscopic phase separation is observed.

CONCLUSIONS

The influence of pressure on the kinetics of mesoglobules formation in aqueous PNIPAM solutions has been investigated with time-resolved SANS following fast pressure changes across the coexistence line, starting in the one-phase region and ending in the two-phase region. The time resolution amounts to ∼50 ms, and a size range of approximately 1−100 nm was covered, which allows unprecedented information on the aggregate sizes, their inner structure, and the growth processes. The elliptical shape of the pressure−temperature coexistence line of aqueous PNIPAM solutions enables pressure jumps at the same temperature at both low and high pressures, thus ruling out thermal effects.

Two series of measurements were carried out, both at 35.1 °C: (i) In the low-pressure regime, pressure jumps from 31 MPa to target pressures in the range of 0.1−20 MPa, and (ii) in the high-pressure regime, pressure jumps from 87 MPa to target pressures in the range of 101−132 MPa. Since the degree of dehydration is much stronger at low pressures than at high pressures, these experiments allow determining the pathway of phase separation under the condition of strong and of weak dehydration. By identifying the roles of the thermodynamic driving force and of kinetic effects, the results contribute to the understanding of mesoglobule formation and their extraordinary stability observed at atmospheric pressure.

In the low-pressure regime, three growth regimes were identified. Immediately after the jumps, the collapse of the chains and their aggregation lead to the formation of fractal clusters. While these clusters first grow by diffusion-limited coalescence, this process is hindered by the viscoelastic effect at later times: The dehydration of the mesoglobules leads to a dense shell, which prevents the interpenetration of chains from different mesoglobules and thereby their coalescence. Thus, the late-stage growth of the mesoglobules is mainly limited by kinetic effects. The duration of each stage depends on the amplitude of the jump. For large-amplitude jumps, the thermodynamic driving force is high, and dehydration proceeds rapidly. The duration of the growth by diffusion-limited coalescence is therefore short, and the slow growth mode sets in earlier. As a result, the mesoglobules form abruptly after the jump but stay relatively small and compact. In contrast, for small-amplitude jumps, only two processes are observed: After slow cluster formation, a stage of slow growth sets in that

DOI: 10.1021/acs.macromol.9b00937
Macromolecules 2019, 52, 6416−6427

continues until the end of the measurement. In this case, the thermodynamic driving force is low, and the growth of the mesoglobules is limited by thermodynamic effects.

In the high-pressure regime, the time-resolved SANS data reveal different growth processes: The PNIPAM chains do not dehydrate as strongly as at low pressures, and mesoglobule growth can proceed via diffusion-limited coalescence, unhindered by the viscoelastic effect; that is, no energy barrier is present. As a result, at the end of the measurements, the mesoglobules are much larger and contain more water than at atmospheric pressure, in agreement with our previous static structural study.[10]

Comparing the results at low and high pressure, we conclude that chain hydration and the resulting chain mobility, that is, the viscoelastic effect, are key for the growth process and the stability of the mesoglobules. This work demonstrates the possibility to use pressure as a variable to manipulate the formation processes of polymer nanostructures and thereby to tune their final size and structure.

■ ASSOCIATED CONTENT

Supporting Information

The Supporting Information is available free of charge on the ACS Publications website at DOI: 10.1021/acs.macromol.9b00937.

Determination of the cloud points. Modeling of SANS data. Energy barriers for coalescence in the LP regime (PDF)

■ AUTHOR INFORMATION

Corresponding Authors

*E-mail: alfons.schulte@ucf.edu. Phone +1 407-823-5196. Fax +1 407-823-5112 (A.S.).

*E-mail: papadakis@tum.de. Phone +49 89 289 12 447. Fax +49 89 289 12 473 (C.M.P.).

ORCID

Alfons Schulte: 0000-0003-0824-8572

Christine M. Papadakis: 0000-0002-7098-3458

Author Contributions

The manuscript was written through contributions of all authors. All authors have given approval to the final version of the manuscript.

Funding

Financial support by Deutsche Forschungsgemeinschaft (DFG) is gratefully acknowledged (PA 771/22-1). A.S. acknowledges support by an August-Wilhelm Scheer visiting professorship at TU Munich. L.C. thanks Technische Universität Berlin and the ILL for postdoctoral funding though a three-year cooperation agreement. The high-pressure SANS cell was developed within the Integrated Infrastructure Initiative for Neutron Scattering and Muon Spectroscopy (NMI3-II) supported by the EU 7th Framework Programme (FP7). The open access fee was covered by FILL2030, a European Union project within the European Commission's Horizon 2020 Research and Innovation programme under grant agreement N°731096.

Notes

The authors declare no competing financial interest.

■ ACKNOWLEDGMENTS

We acknowledge ILL for allocation of beamtime at instrument D11 (DOI:10.5291/ILL-DATA.9-11-1827) and the support of the sample environment (SANE) and the instrument control (SCI) teams of the ILL, in particular C. Payre and J. Maurice.

■ REFERENCES

(1) Tyedmers, J.; Mogk, A.; Bukau, B. Cellular Strategies for Controlling Protein Aggregation. *Nat. Rev. Mol. Cell Biol.* **2010**, *11*, 777−788.

(2) Ditsch, A.; Laibinis, P. E.; Wang, D. I. C.; Hatton, T. A. Controlled Clustering and Enhanced Stability of Polymer-Coated Magnetic Nanoparticles. *Langmuir* **2005**, *21*, 6006−6018.

(3) Kovalchuk, N.; Starov, V.; Langston, P.; Hilal, N. Formation of Stable Clusters in Colloidal Suspensions. *Adv. Colloid Interface Sci.* **2009**, *147-148*, 144−154.

(4) Hecht, F. M.; Bausch, A. R. Kinetically Guided Colloidal Structure Formation. *Proc. Natl. Acad. Sci. U. S. A.* **2016**, *113*, 8577−8582.

(5) Stuart, M. A. C.; Huck, W. T. S.; Genzer, J.; Müller, M.; Ober, C.; Stamm, M.; Sukhorukov, G. B.; Szleifer, I.; Tsukruk, V. V.; Urban, M.; Winnik, F.; Zauscher, S.; Luzinov, I.; Minko, S. Emerging Applications of Stimuli-Responsive Polymer-Materials. *Nat. Mater.* **2010**, *9*, 101−113.

(6) Cabane, E.; Zhang, X.; Langowska, K.; Palivan, C. G.; Meier, W. Stimuli-Responsive Polymers and their Applications in Nanomedicine. *Biointerphases* **2012**, *7*, 9.

(7) Bertrand, O.; Gohy, J.-F. Photo-Responsive Polymers: Synthesis and Applications. *Polym. Chem.* **2017**, *8*, 52−73.

(8) Wei, M.; Gao, Y.; Li, X.; Serpe, M. J. Stimuli-Responsive Polymers and their Applications. *Polym. Chem.* **2017**, *8*, 127−143.

(9) Halperin, A.; Kröger, M.; Winnik, F. M. Poly(*N*-isopropylacrylamide) Phase Diagrams: Fifty Years of Research. *Angew. Chem., Int. Ed.* **2015**, *54*, 15342−15367.

(10) Niebuur, B.-J.; Claude, K.-L.; Pinzek, S.; Cariker, C.; Raftopoulos, K. N.; Pipich, V.; Appavou, M.-S.; Schulte, A.; Papadakis, C. M. Pressure-Dependence of Poly(*N*-isopropylacrylamide) Mesoglobule Formation in Aqueous Solution. *ACS Macro Lett.* **2017**, *6*, 1180−1185.

(11) Niebuur, B.-J.; Lohstroh, W.; Appavou, M.-S.; Schulte, A.; Papadakis, C. M. Water Dynamics in a Concentrated Poly(*N*-isopropylacrylamide) Solution at Variable Pressure. *Macromolecules* **2019**, *52*, 1942−1954.

(12) Wu, C.; Wang, X. Globule-to-Coil Transition of a Single Homopolymer Chain in Solution. *Phys. Rev. Lett.* **1998**, *80*, 4092−4094.

(13) Okada, Y.; Tanaka, F. Cooperative Hydration, Chain Collapse, and Flat LCST Behavior in Aqueous Poly(*N*-isopropylacrylamide) Solutions. *Macromolecules* **2005**, *38*, 4465−4471.

(14) de Gennes, P. G. Kinetics of Collapse for a Flexible Coil. *J. Phys., Lett.* **1985**, *46*, 639−642.

(15) Grosberg, A. Y.; Nechaev, S. K.; Shakhnovich, E. I. The Role of Topological Constraints in the Kinetics of Collapse of Macromolecules. *J. Phys. France* **1988**, *49*, 2095−2100.

(16) Dawson, K. A.; Timoshenko, E. G.; Kiernan, P. Theoretical and Experimental Approaches to Kinetics at the Collapse Transition of a Homopolymer. *Il Nuovo Cimento D* **1994**, *16*, 675−687.

(17) Xu, J.; Zhu, Z.; Luo, S.; Wu, C.; Liu, S. First Observation of Two-Stage Collapsing Kinetics of a Single Synthetic Polymer Chain. *Phys. Rev. Lett.* **2006**, *96*, 027802.

(18) Ye, X.; Lu, Y.; Shen, L.; Ding, Y.; Liu, S.; Zhang, G.; Wu, C. How Many Stages in the Coil-to-Globule Transition of Linear Homopolymer Chains in a Dilute Solution? *Macromolecules* **2007**, *40*, 4750−4752.

(19) Li, C.; Ye, X.; Ding, Y.; Liu, S. Kinetics of Coil-to-Globule Transition of Dansyl-Labeled Poly(*N*-isopropylacrylamide) Chains in Aqueous Solution. *Chin. J. Chem. Phys.* **2012**, *25*, 389−397.

(20) Lu, Y.; Ye, X.; Li, J.; Li, C.; Liu, S. Kinetics of Laser-Heating-Induced Phase Transition of Poly(*N*-isopropylacrylamide) Chains in Dilute and Semidilute Solutions. *J. Phys. Chem. B* **2011**, *115*, 12001−12006.

(21) Aseyev, V.; Hietala, S.; Laukkanen, A.; Nuopponen, M.; Confortini, O.; Du Prez, F. E.; Tenhu, H. Mesoglobules of

DOI: 10.1021/acs.macromol.9b00937
Macromolecules 2019, 52, 6416−6427

Thermoresponsive Polymers in Dilute Aqueous Solutions Above the LCST. *Polymer* **2005**, *46*, 7118−7131.
(22) Kujawa, P.; Aseyev, V.; Tenhu, H.; Winnik, F. M. Temperature-Sensitive Properties of Poly(*N*-isopropylacrylamide) Mesoglobules Formed in Dilute Aqueous Solutions Heated Above their Demixing Point. *Macromolecules* **2006**, *39*, 7686−7693.
(23) Maresov, E. A.; Semenov, A. N. Mesoglobule Morphologies of Amphiphilic Polymers. *Macromolecules* **2008**, *41*, 9439−9457.
(24) Gorelov, A. V.; Du Chesne, A.; Dawson, K. A. Phase Separation in Dilute Solutions of Poly(*N*-isopropylacrylamide). *Phys. A* **1997**, *240*, 443−452.
(25) Chan, K.; Pelton, R.; Zhang, J. On the Formation of Colloidally Dispersed Phase-Separated Poly(*N*-isopropylacrylamide). *Langmuir* **1999**, *15*, 4018−4020.
(26) Balu, C.; Delsanti, M.; Guenoun, P.; Monti, F.; Cloitre, M. Colloidal Phase Separation of Concentrated PNIPAm Solutions. *Langmuir* **2007**, *23*, 2404−2407.
(27) Wu, C.; Li, W.; Zhu, X. X. Viscoelastic Effect on the Formation of Mesoglobular Phase in Dilute Solutions. *Macromolecules* **2004**, *37*, 4989−4992.
(28) Vasilevskaya, V. V.; Khalatur, P. G.; Khokhlov, A. R. Conformational Polymorphism of Amphiphilic Polymers in a Poor Solvent. *Macromolecules* **2003**, *36*, 10103−10111.
(29) Laukkanen, A.; Valtola, L.; Winnik, F. M.; Tenhu, H. Formation of Colloidally Stable Phase Separated Poly(*N*-vinylcaprolactam) in Water: A Study by Dynamic Light Scattering, Microcalorimetry, and Pressure Perturbation Calorimetry. *Macromolecules* **2004**, *37*, 2268−2274.
(30) Zhang, G.; Wu, C.Folding and Formation of Mesoglobules in Dilute Copolymer Solutions. In *Conformation-Dependent Design of Sequences in Copolymers I. Advances in Polymer Science*, vol *195*, Springer Berlin: Heidelberg, 2006.
(31) Tanaka, H. Viscoelastic Phase Separation. *J. Phys.: Condens. Matter* **2000**, *12*, 207−264.
(32) Chuang, J.; Grosberg, A. Y.; Tanaka, T. Topological Repulsion Between Polymer Globules. *J. Chem. Phys.* **2000**, *112*, 6434−6442.
(33) Meier-Koll, A.; Pipich, V.; Busch, P.; Papadakis, C. M.; Müller-Buschbaum, P. Phase Separation in Semidilute Aqueous Poly(*N*-isopropylacrylamide) Solutions. *Langmuir* **2012**, *28*, 8791−8798.
(34) Lu, Y.; Ye, X.; Zhou, K.; Shi, W. A Comparative Study of Urea-Induced Aggregation of Collapsed Poly(*N*-isopropylacrylamide) and Poly(*N*,*N*-diethylacrylamide) Chains in Aqueous Solutions. *J. Phys. Chem. B* **2013**, *117*, 7481−7488.
(35) Meersman, F.; Wang, J.; Wu, Y.; Heremans, K. Pressure Effect on the Hydration Properties of Poly(*N*-isopropylacrylamide) in Aqueous Solution Studied by FTIR Spectroscopy. *Macromolecules* **2005**, *38*, 8923−8928.
(36) Dadarlat, V. M.; Post, C. B. Decomposition of Protein Experimental Compressibility into Intrinsic and Hydration Shell Contributions. *Biophys. J.* **2006**, *91*, 4544−4554.
(37) Smolin, N.; Winter, R. A Molecular Dynamics Simulation of SNase and its Hydration Shell at High Temperature and High Pressure. *Biochim. Biophys. Acta* **2006**, *1764*, 522−534.
(38) Sarupria, S.; Garde, S. Quantifying Water Density Fluctuations and Compressibility of Hydration Shells of Hydrophobic Solutes and Proteins. *Phys. Rev. Lett.* **2009**, *103*, No. 037803.
(39) Grigera, J. R.; McCarthy, A. N. The Behavior of the Hydrophobic Effect under Pressure and Protein Denaturation. *Biophys. J.* **2010**, *98*, 1626−1631.
(40) Mochizuki, K.; Sumi, T.; Koga, K. Driving Forces for the Pressure-Induced Aggregation of Poly(*N*-isopropylacrylamide) in Water. *Phys. Chem. Chem. Phys.* **2016**, *18*, 4697−4703.
(41) Niebuur, B.-J.; Chiappisi, L.; Zhang, X.; Jung, F.; Schulte, A.; Papadakis, C. M. Formation and Growth of Mesoglobules in Aqueous Poly(*N*-isopropylacrylamide) Solutions Revealed with Kinetic Small-Angle Neutron Scattering and Fast Pressure Jumps. *ACS Macro Lett.* **2018**, *7*, 1155−1160.
(42) Mencke, A.; Cheng, A.; Caffrey, M. A Simple Apparatus for Time-Resolved X-ray Diffraction Biostructure Studies using Static and Oscillating Pressures and Pressure Jumps. *Rev. Sci. Instrum.* **1993**, *64*, 383−389.
(43) Steinhart, M.; Kriechbaum, M.; Pressl, K.; Amenitsch, H.; Laggner, P.; Bernstorff, S. High-Pressure Instrument for Small- and Wide-Angle X-ray Scattering. II. Time-Resolved Experiments. *Rev. Sci. Instrum.* **1999**, *70*, 1540−1545.
(44) Woenckhaus, J.; Köhling, R.; Winter, R.; Thiyagarajan, P.; Finet, S. High Pressure-Jump Apparatus for Kinetic Studies of Protein Folding Reactions using the Small-Angle Synchrotron X-ray Scattering Technique. *Rev. Sci. Instrum.* **2000**, *71*, 3895−3899.
(45) Brooks, N. J.; Gauthe, B. L. L. E.; Terrill, N. J.; Rogers, S. E.; Templer, R. H.; Ces, O.; Seddon, J. M. Automated High Pressure Cell for Pressure Jump X-ray Diffraction. *Rev. Sci. Instrum.* **2010**, *81*, No. 064103.
(46) Clegg, R. M.; Maxfield, B. W. Chemical Kinetic Studies by a New Small Pressure Perturbation Method. *Rev. Sci. Instrum.* **1976**, *47*, 1383−1393.
(47) Pearson, D. S.; Holtermann, G.; Ellison, P.; Cremo, C.; Geeves, M. A. A Novel Pressure-Jump Apparatus for the Microvolume Analysis of Protein-Ligand and Protein-Protein Interactions: its Application to Nucleotide Binding to Skeletal-Muscle and Smooth-Muscle Myosin Subfragment-1. *Biochem. J.* **2002**, *366*, 643−651.
(48) Möller, J.; Léonardon, J.; Gorini, J.; Dattani, R.; Narayanan, T. A Sub-ms Pressure Jump Setup for Time-Resolved X-Ray Scattering. *Rev. Sci. Instrum.* **2016**, *87*, 125116.
(49) Kunugi, S.; Yamazaki, Y.; Takano, K.; Tanaka, N.; Akashi, M. Effects of Ionic Additives and Ionic Comonomers on the Temperature and Pressure Responsive Behavior of Thermoresponsive Polymers in Aqueous Solutions. *Langmuir* **1999**, *15*, 4056−4061.
(50) Kunugi, S.; Tanaka, N. Cold Denaturation of Proteins Under High Pressure. *Biochim. Biophys. Acta* **2002**, *1595*, 329−344.
(51) Ebeling, B.; Eggers, S.; Hendrich, M.; Nitschke, A.; Vana, P. Flipping the Pressure- and Temperature-Dependent Cloud-Point Behavior in the Cononsolvency System of Poly(*N*-isopropylacrylamide) in Water and Ethanol. *Macromolecules* **2014**, *47*, 1462−1469.
(52) Shibayama, M.; Tanaka, T.; Han, C. C. Small Angle Neutron Scattering Study on Poly(*N*-isopropyl acrylamide) Gels Near Their Volume-Phase Transition Temperature. *J. Chem. Phys.* **1992**, *97*, 6829−6841.
(53) Teraoka, I. *Polymer Solutions: An Introduction to Physical Properties*; Wiley-Interscience: New York, 2002.
(54) Hammouda, B.; Ho, D.; Kline, S. SANS from Poly(ethylene oxide)/Water Systems. *Macromolecules* **2002**, *35*, 8578−8585.
(55) Hammouda, B.; Ho, D. L.; Kline, S. Insight into Clustering in Poly(ethylene oxide) Solutions. *Macromolecules* **2004**, *37*, 6932−6937.
(56) Hammouda, B. A New Guinier-Porod Model. *J. Appl. Crystallogr.* **2010**, *43*, 716−719.
(57) Koberstein, J. T.; Morra, B.; Stein, R. S. The Determination of Diffuse-Boundary Thicknesses of Polymers by Small-Angle X-ray Scattering. *J. Appl. Crystallogr.* **1980**, *13*, 34−45.
(58) Ciccariello, S.; Goodisman, J.; Brumberger, H. On the Porod Law. *J. Appl. Crystallogr.* **1988**, *21*, 117−128.
(59) Porod, G. Die Röntgenkleinwinkelstreuung von dichtgepackten kolloiden Systemen. *Kolloid-Z.* **1951**, *124*, 83−114.
(60) Grillo, I. Small-Angle Neutron Scattering and Applications in Soft Condensed Matter. In *Soft-Matter Characterization*; Borsali, R., Pecora, R., Eds.; Springer: Dordrecht, The Netherlands, 2008.
(61) Kujawa, P.; Winnik, F. M. Volumetric Studies of Aqueous Polymer Solutions Using Pressure Perturbation Calorimetry: A New Look at the Temperature-Induced Phase Transition of Poly(*N*-isopropylacrylamide) in Water and D_2O. *Macromolecules* **2001**, *34*, 4130−4135.
(62) Yuan, G.; Wang, X.; Han, C. C.; Wu, C. Reexamination of Slow Dynamics in Semidilute Solutions: From Correlated Concentration Fluctuation to Collective Diffusion. *Macromolecules* **2006**, *39*, 3642−3647.
(63) Shibayama, M.; Isono, K.; Okabe, S.; Karino, T.; Nagao, M. SANS Study on Pressure-Induced Phase Separation of Poly(*N*-

DOI: 10.1021/acs.macromol.9b00937
Macromolecules 2019, 52, 6416−6427

isopropylacrylamide) Aqueous Solutions and Gels. *Macromolecules* **2004**, *37*, 2909−2918.
(64) Stepanyan, R.; Lebouille, J. G. J. L.; Slot, J. J. M.; Tuinier, R.; Stuart, M. A. C. Controlled Nanoparticle Formation by Diffusion Limited Coalescence. *Phys. Rev. Lett.* **2012**, *109*, 138301.
(65) Maeda, Y.; Higuchi, T.; Ikeda, I. Change in Hydration State during the Coil-Globule Transition of Aqueous Solutions of Poly(*N*-isopropylacrylamide) as Evidenced by FTIR Spectroscopy. *Langmuir* **2000**, *16*, 7503−7509.
(66) Philipp, M.; Kyriakos, K.; Silvi, L.; Lohstroh, W.; Petry, W.; Krüger, J. K.; Papadakis, C. M.; Müller-Buschbaum, P. From Molecular Dehydration to Excess Volumes of Phase-Separating PNIPAM Solutions. *J. Phys. Chem. B* **2014**, *118*, 4253−4260.

DOI: 10.1021/acs.macromol.9b00937
Macromolecules 2019, 52, 6416−6427